Check for updates

High resolution upper crustal velocity and seismogenic structure of the Huoshan "seismic window" in the Dabie orogenic belt

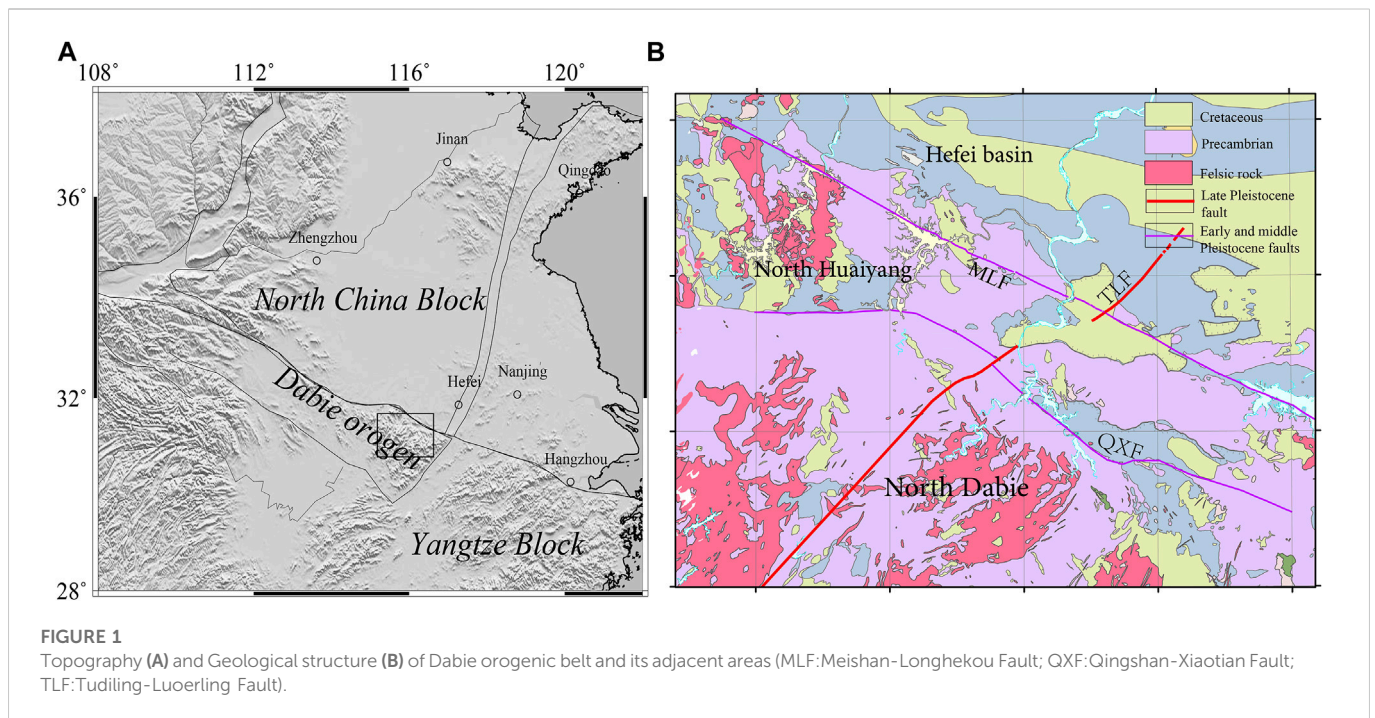Lingli Li[1,2]*, Huajian Yao[3,2], Bing Zhang[1,2], Junhui Li[1,2], Peng Shu[1,2], Yuanyuan Yang[1,2], Xiaoli Wang[1,2], Dongrui Zhou[1,2], Peng Zhao[1,2] and Jiaji Luo[1,2]

[1]Anhui Earthquake Administration, Hefei, China, [2]Anhui Mengcheng National Geophysical Observatory, Mengcheng, Anhui, China, [3]Laboratory of Seismology and Physics of Earth's Interior, School of Earth and Space Sciences, University of Science and Technology of China, Hefei, China

Huoshan "seismic window" is located in the northern margin of the Dabie Orogen belt, the contact zone between North China and the Yangtze plate, where the seismic activity is mainly concentrated in this area. Small earthquake swarms in this region often appear before significant moderate-strong earthquakes in East China. To reveal the fine structures of several faults and discuss their correlation with the seismic activity, a seismic array composed of 136 sets of short period seismometers was deployed in the Huoshan region and its surrounding areas. Ambient noise data were recorded for 1 month, and a 3-D velocity structure model of the upper crust was constructed. The results show that with the Meishan-Longhekou and Qingshan-Xiaotian faults as the boundary, the Dabie Mountain, Hefei Basin, North Dabie and North Huaiyang show exhibit obvious high and low velocity variation characteristics. The shallow crust along the NW-trending, normal Qingshan-Xiaotian fault, presents a high velocity zonal distribution, which is related to the large number of magmatic and metamorphic rocks exposed under the strong metamorphic power in this region. The NE-trending Tudiling-Luoerling fault comprised three groups of parallel and nearly vertical en echelon secondary faults in the upper crust, which control most of the seismic activities. A relatively low velocity anomaly is observed in the seismic concentrated occurrence layer near the intersection of the fault. It suggests that this area inherits the property of the low velocity detachment zone of the middle crust in the wing of the Dabie Mountain dome structure, and a relatively broken weak structural zone form near the intersection of the fault, which leads to the release of small strain accumulation, thus enriching small earthquake activities. The focal depth of earthquakes above ML3 mainly distribute along the Tudiling-Luoerling fault plane, which is indicated this fault is the main seismogenic fault of greater seismicity in Huoshan "seismic window". This study provides an important model basis for reliable earthquake location, focal mechanism and the determination of possible earthquake risk sites, and provides a reference for the further study of small earthquake activity mechanism of other "seismic windows" in China.

KEYWORDS

shallow velocity structure, dense seismic array, seismicity, Huoshan "seismic window", seismogenic structure

FIGURE 1
Topography **(A)** and Geological structure **(B)** of Dabie orogenic belt and its adjacent areas (MLF:Meishan-Longhekou Fault; QXF:Qingshan-Xiaotian Fault; TLF:Tudiling-Luoerling Fault).

1 Introduction

There are some regions in mainland China where small and medium-sized earthquakes are very active, and the frequency of their seismic activity over time is indicative of moderate-to-strong earthquakes in the corresponding regions, so they are called "seismic windows". For many years, the statistical characteristics of the seismic activity of "seismic windows" have become one of the main indicators for the assessment of seismic hazard (routine work) in mainland China. However, the seismogenic mechanism, subsurface tectonic characteristics and velocity structure of the "seismic window" have not been studied in depth, and the physical significance of the seismic activity of the "seismic window" cannot be deeply understood. The Huoshan area studied in this paper is such a "seismic window".

The Huoshan area is located in the northeastern margin of the Dabie Mountains and is adjacent to the Tanlu Fault Zone in the east. It is the most concentrated and active area of seismic activity in the Dabie Mountains and surrounding areas. Many groups of crisscross faults exist in the area, the most important of which are the NE-trending Tudiling-Luoerling fault (TLF) and the NW-trending Qingshan-Xiaotian fault (QXF; Figure 1) Small earthquakes (below ML3) have been very active in the modern era (since 1970) since instrumental records were available and have repeatedly shown near-periodic small-earthquake swarm activity before the occurrence of medium-strong earthquakes in East China (l_1). It is suggested that the eastward extrusion of crustal materials caused by the convergence of tectonic plates, with the consequence of strong seismic activity in western China. The driving force of the crustal extrusion also can be transmitted to eastern China along the Qinling-Dabie orogenic belt As a result, in the Huoshan area where is the intersection of multiple groups of faults, small eartthquke swarms are active, and small earthquakes swarms are active before the occurrences of some moderate-strong earthquakes in eastern China (Hong et al., 2013; Miao et al., 2014). In earthquake prediction research (Routine work in China Earthquake Administration), the cumulative frequency of Huoshan "seismic window" earthquake activity with ML1.0 or above in 3 months has reached more than 40, which is often used as an index for earthquake prediction within a certain range.

In addition to the active concentration of small earthquakes, the spatial characteristics of historical earthquakes of magnitude 5 or higher in the region are also obvious, mostly spreading along the Tudiling-Luoerling fault, with the maximum magnitude of 6.25 in 1917. However, there are few earthquakes with the magnitude above 5 in the concentrated area of small earthquakes. A remarkable characteristic of seismic activity is that the spatial distribution of historically strong earthquakes is quite different from that of modern small earthquakes, which is closely related to the characteristics and control of the regional fault structure. Therefore, in-depth research on the seismotectonic characteristics of the Huoshan "seismic window" and the correlation with seismic activity is important for understanding the causes of small earthquake swarms and the mechanism of fault inception and earthquake risk prediction in the Dabie orogenic belt.

Geological researches show that the Tudiling-Luoerling fault has been an active fault since the early Late Pleistocene in the Dabie area (Yao et al., 2003; Shu et al., 2018), with a tectonic background of strong earthquake activity. However, because the historical earthquakes are only written records, there is no evidence of surface rupture even for the 6.25 strong earthquake in 1917. Therefore, the research on the seismogenic structure of the fault is insufficient. An Ms4.3 earthquake struck the Huoshan area in 2014, with the epicenter close to the southern side of the Qingshan-Xiaotian fault. This is the largest earthquake in the region in the past 50 years. The focal mechanism solution results show that the earthquake occurred due to a typical right-lateral strike-slip movement of the tectonic plates, which is related to the horizontal compression in the east-west direction and the horizontal tension in the north-south direction in the Huoshan area (Liu et al., 2015). However, the two nodal results of the focal mechanism solution cannot determine which fault is the main seismogenic structure. Cui et al. (2020) believed that the seismogenic fault of the earthquake was the Tudiling-Luoerling fault through the

electrical structure, but the resolution of the Qingshan-Xiaotian fault was not sufficient. Xu et al. (2022) used the regional stress field to simulate and calculate three NE-trending seismic sections and suggested that the main earthquake-controlling fault in the region is the NE-trending Tuling-Luoerling fault. However, detailed fine structural differences between the two faults in the Huoshan area and their relation with seismic activity require more geophysical observation evidence.

Seismotectonic characteristics affect the preparation and occurrence of earthquakes. Therefore, the fine geometric shape of faults needs to be studied to provide an important modeling basis for accurate localization of regional earthquakes, research on seismogenic mechanisms, and determination of earthquake hazard locations. The main body of small and medium earthquakes is concentrated in the intersection of the two faults, and the focal depth is mostly shallow than 10 km. Therefore, the study of the fine velocity structure of the upper crust can provide a reference for the seismogenic mechanism in this area.

Previous studies have obtained the high-resolution structural model of the Chinese mainland by the joint inversion of seismic body waves and surface waves (Xin et al., 2019; Han et al., 2022) and of the region around the Dabie Mountains (Luo et al., 2013; Ye, et al., 2015; Xiong et al., 2019), providing important deep velocity structure information for determining the tectonic evolution dynamics of the Dabie orogenic belt. Early studies of several artificial seismic deep reflection profiles and other geophysical data have also systematically revealed the dynamic characteristics of the crust-mantle structure and the deep tectonic evolution beneath the Dabie Mountains (Dong, 1999; Dong et al., 2005; Zhang et al., 2000; Yang, 2003; Xu et al., 2000; Xiao et al., 2007; Liu et al., 2003; Yuan et al., 2003). However, for studying the small-scale structure of the Huoshan seismic zone in the northern margin of the Dabie Mountain, data on the fine structure characteristics of multiple sets of faults are still lacking, especially on the seismogenic environment associated with seismic activity. In terms of the detection method of the regional fine velocity structure, currently, through dense array observation, a fault-scale fine model of fault scale can be constructed. Consequently, the lateral resolution of inversion can reach the order of several kilometers or even hundreds of meters (Yao, 2020), which provides more constraints for the fine structure of the upper crust seismogenic layer and reveals the control effect of the regional faults on seismic activity.

To elucidate the structural characteristics of the possible seismogenic layer beneath the two main faults in Huoshan area and study its tectonic correlation with seismic activity, this study uses the ambient noise data recorded by a dense array of 136 short-period seismometers in the Huoshan area to construct a high-resolution velocity structure of the upper crust at the depths of 1–7.5 km, improving the resolution accuracy of the seismic concentration area. Furthermore, combined with the results of the small earthquake relocation, the seismogenic structure and seismogenic environment in the deep crust beneath the Huoshan "seismic window" are discussed.

2 Data and methods

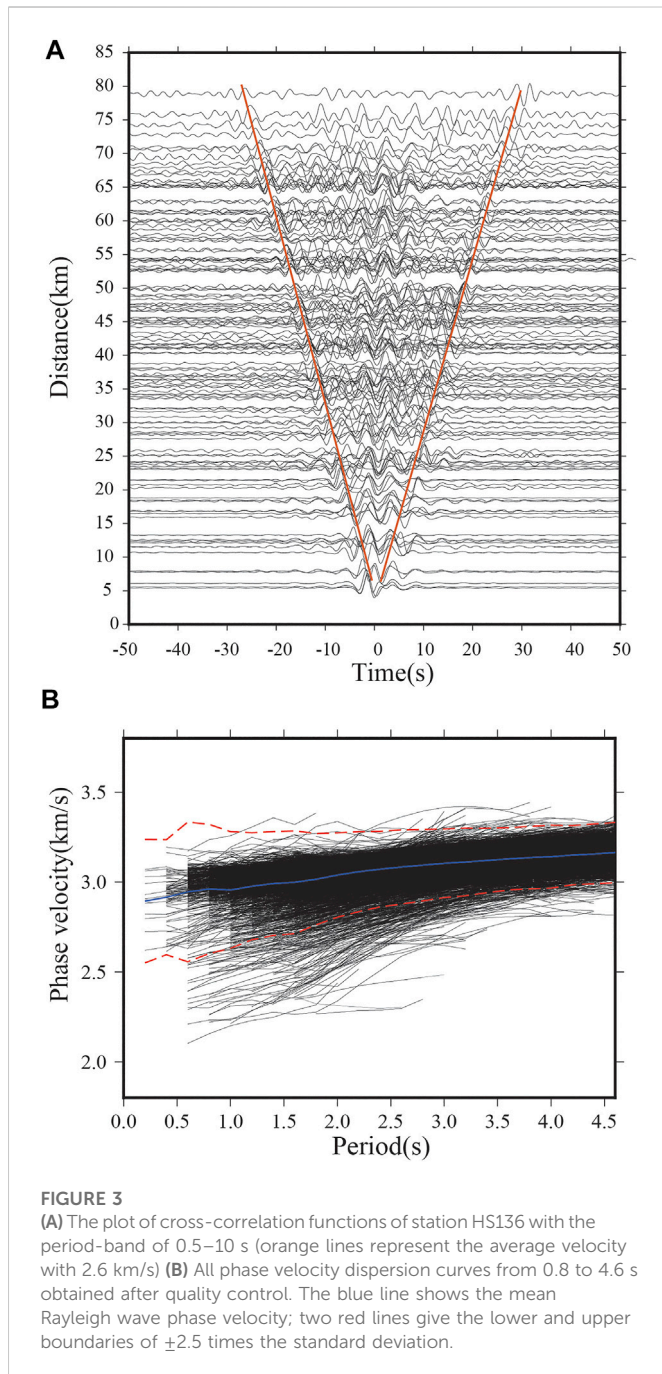## 2.1 Data processing and dispersion measurements

The data used in our study comprise continuous data records of the vertical component of ambient noise collected from 26 April 2021 to 6 June 2021 by 136 short-period temporary seismometers deployed around Huoshan and the adjacent areas (Figure 2). The data
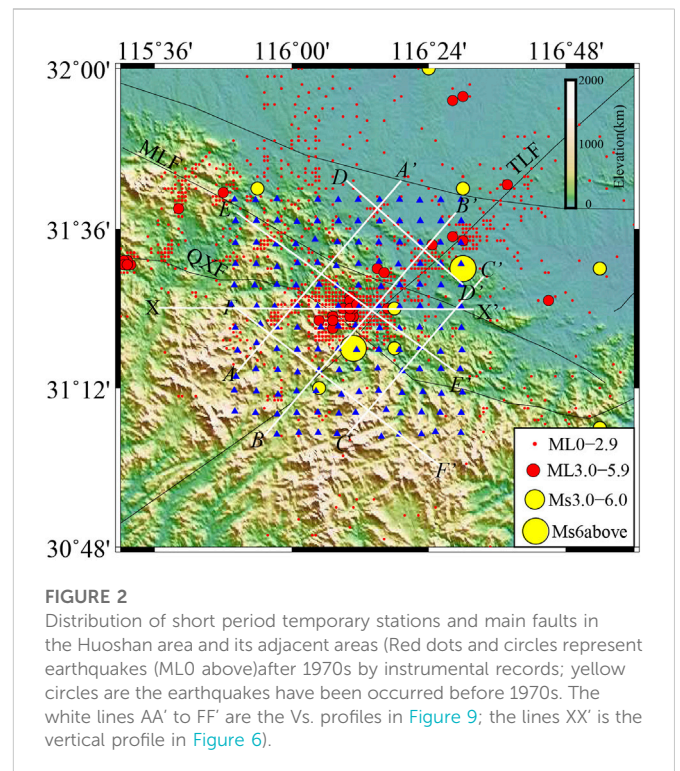
FIGURE 2
Distribution of short period temporary stations and main faults in the Huoshan area and its adjacent areas (Red dots and circles represent earthquakes (ML0 above)after 1970s by instrumental records; yellow circles are the earthquakes have been occurred before 1970s. The white lines AA' to FF' are the Vs. profiles in Figure 9; the lines XX' is the vertical profile in Figure 6).

were classified into daily records and then subjected to various forms of data processing, which aims to improve the signal-to-noise ratio (SNR) or suppress strong instantaneous signals. The entire date processing process can be found in Bensen et al. (2007). The daily data of each station were decimated and re-sampled at 20 Hz before detrending and demeaning. Then, to eliminate the influences of fixed noise sources, the data were segmented into multiple time series in three connecting period bands (0.5–2, 2–5, 5–10 s) and temporal normalization was performed for each band. The different period bands were finally stacked to afford normalized daily broadband (0.5–10 s) waveforms for the daily station-pair cross-correlation. Finally, the noise cross-correlation functions (NCFs) were obtained from 9180 station pairs, and EGFs were computed from the NCFs (NCFs between station 136 and others shown in Figure 3A).

The image transforms analysis technique of Yao et al. (2006,2011) was employed to extract the fundamental mode Rayleigh wave group and phase velocity dispersion curves from the EGF of every station pair. About 4244 phase dispersion curves were selected following several quality control criteria: 1) The SNR>4; 2) deviation greater than 2.5; and 3) small differences on similar paths. Subsequently, 4242 reliable phase dispersion curves were finally selected for direct inversion for this study. Figure 3B shows that the phase velocity varies significantly from 2.2 km/s to 3.2 km/s in the period band of 0.6–2 s, revealing the strong lateral heterogeneity of the shallow crust. Due to the small changes of dispersion in the long period, the short period instrument may have poor sensitivity. Thus, reliable phase velocity dispersion curves with a period of 0.8–4.6 s were selected for the direct inversion for the high-resolution three-dimensional (3D) tomography (Figure 3B).

FIGURE 4
1-D depth sensitivity kernels to Vs. for the Rayleigh wave fundamental phase velocity at different periods using the average velocity.

FIGURE 3
(A) The plot of cross-correlation functions of station HS136 with the period-band of 0.5–10 s (orange lines represent the average velocity with 2.6 km/s) **(B)** All phase velocity dispersion curves from 0.8 to 4.6 s obtained after quality control. The blue line shows the mean Rayleigh wave phase velocity; two red lines give the lower and upper boundaries of ±2.5 times the standard deviation.

2.2 Inversion method for 3-D vs. structure

In this study, the direct surface wave tomography method (DSurfTomo) of Fang et al. (2015) was employed to obtain a fine 3-D shear wave velocity model of the upper crust in the Huoshan area and adjacent areas. Considering the influence of bending rays of complex medium paths with smaller scales in the Huoshan area, the inversion problem was solved using the ray fast tracing method (Paige and Saunders, 1982; Rawlinson and Sambridge, 2005). This method skips the intermediate step of computing two-dimensional phase velocity maps that are based on the assumption of a great circle distance between the stations.

The average one-dimensional shear velocity model was fabricated from all the dispersion data from the depths of 0–5 km, and Luo's
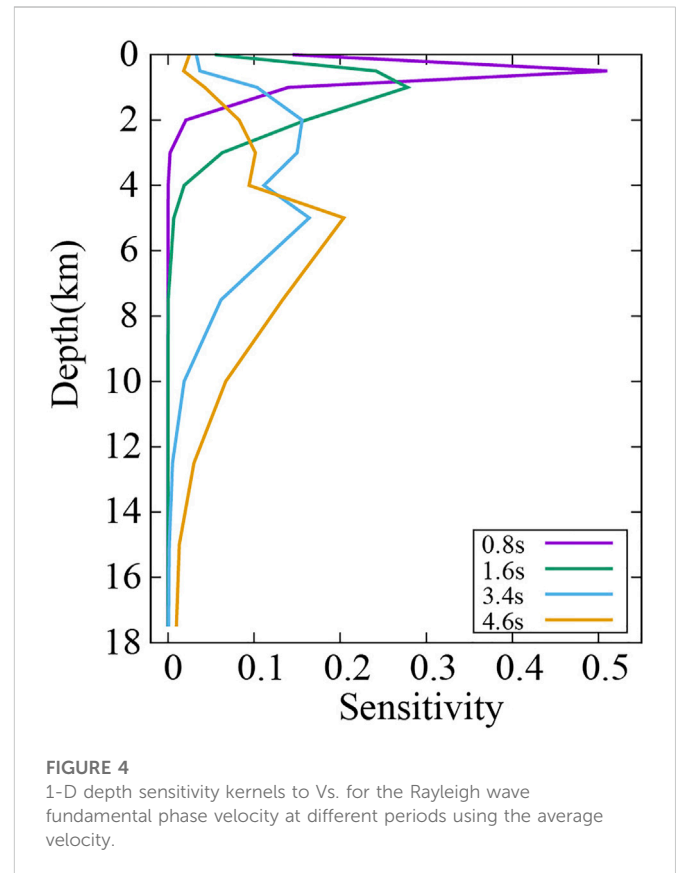
crustal velocity model (Luo et al., 2019) from the dispersion data from the depths of 5–15 km was constructed as an initial velocity model. A 0.04°×0.04° grid interval in the horizontal directions was employed, yielding 16×13 and 11 depth grid points. The depth grid intervals were kept constant at 0.5 km from the surface to 2 km and increased to 1 km and 2.5 km at the depths of 2–5 km and 5–15 km, respectively. The checkboard test was used to access the model resolution in 3D. First, a synthetic model was generated, producing positive and negative checkerboard anomalies with a size of 0.08°×0.08°. Second, 2% Gaussian random noise was considered for the synthetic travel time data and inverted using exactly the same parameters and the number of iterations as those used for the inversion of the real data. After five iterations, the inversion results tended to stabilize, and the RMS decreased from 0.48 to 0.192 (Supplementary Figure S1). We rely on the Rayleigh wave depth sensitivity kernels of the periods from 0.8 to 4.6 s to constrain the reliable depth range for our results. Such depth sensitivity information is often obtained from the 1-D depth sensitivity kernels for Rayleigh waves. The kernels for some periods (0.6 s,1.6 s,3.4 s, 4.6 s) (Figure 4) show that the depth sensitivity increasing with increasing periods. The shallow part of the uppermost crust (<2 km) is constrained by the 0.8 s period, while the 4.6 s period is mainly sensitive to the lower brittle part of the upper crust (5–8 km). The sensitivity kernels reveal that our dataset is capable of resolving features in upper crust in this study.

The results are shown as horizontal slices in Figure 5 and vertical slices (herein, only the vertical profile (shown in Figure 2 X-X') for the latitude equals to 31.4° was tested in Figure 6. The velocity anomalies are well resolved by the dense crisscrossing ray paths (Figure 7) in the depth range of 1–7.5 km.
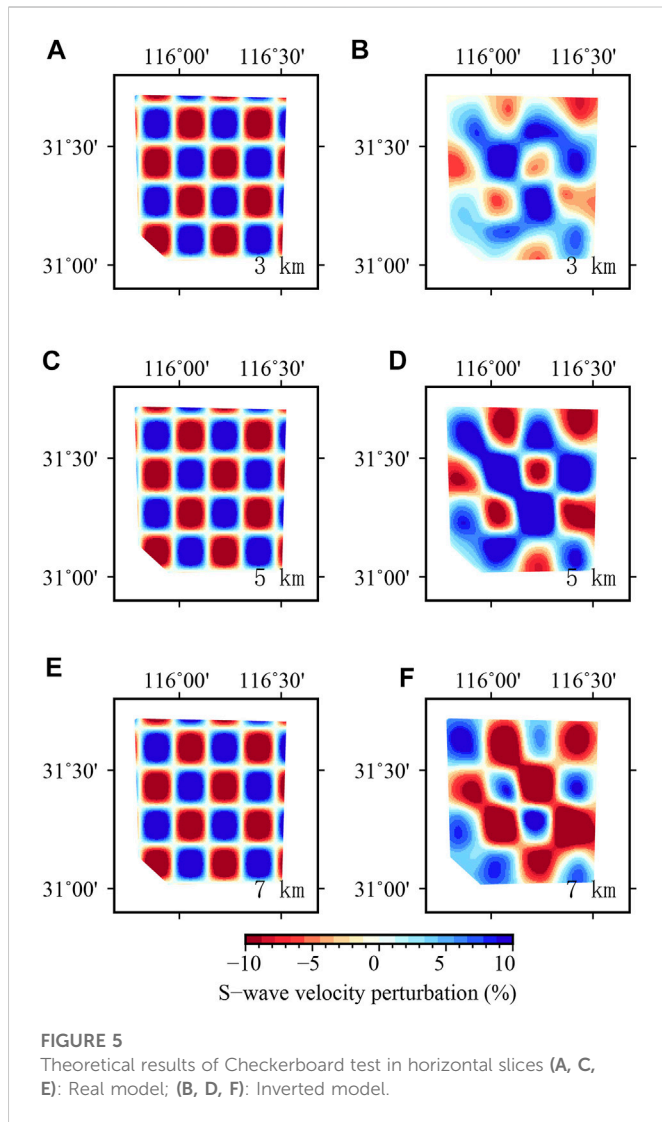
3 Results

Figure 8 displays the shear wave velocities at different depths (1–7.5 km) in the Huoshan earthquake area and adjacent areas (31–31.7°N, 115.8–116.5°E). Slices with different depths reveal the obvious high and low velocity conversions of the Dabie Mountains and Hefei Basin. The velocity structures relatively correspond to the geological and geomorphic characteristics of known tectonic units, which is consistent with the large-scale results of the region obtained by Luo et al. (2019). However, the results of this study depict more detailed information of multiple groups of faults. The details are as follows:

3.1 The NW-trending high velocity anomaly on the northern edge of the Dabie mountains

The northern edge of the Dabie Mountains has a high velocity anomaly in the shallow crust (Figure 8A, B), and has a relatively obvious zonal distribution along the NW direction, which is consistent with the trend of the Meishan-Longhekou and Qingshan-Xiaotian faults in this area, indicating the structural characteristics of the northern border fault of the Dabie Mountains. This figure shows that the NW-trending fractures
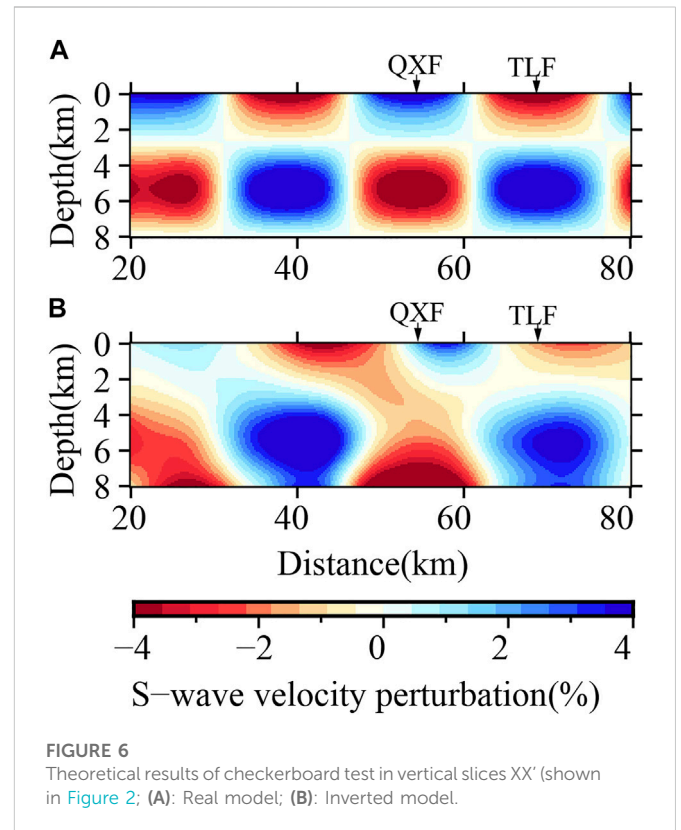
have a certain control over the linear distribution of several high-velocity anomaly bodies. The value in the high velocity region is more than 3.6 km/s near the surface, which is similar to the velocity value obtained by Luo et al. (2012, 2013) in the shallow crust. The Qingshan-Xiaotian fault is the northern boundary of the North Dabie with complex rocks (Wang et al., 2009), and weak Quaternary development. The Yuexi-Yingshan area to the south is a concentrated zoneof high/ultrahigh pressure metamorphic rocks (Xiao et al., 2007). The North Dabie comprises complex metamorphic rocks and abundant Yanshanian granites (Jiang et al., 2000). Strong magnetic intrusive rocks and pyroclastic sedimentary rock series are developed on the surface of the North Huaiyang (Du and Zhang, 1999; Liu et al., 2010; Wang et al., 2012), which is consistent with the high anomaly features near the faults in this area. From the surface to 2 km depth, the NW-trending high velocity is more prominent in the shallow crust, which is consistent with the geomorphic features (Zhao et al., 2018) of the broken rock mass exposed along the Qingshan-Xiaotian fault, as well as the shallow metamorphic rocks of the Foziling Group in the Huoshan area (Liu Y C et al., 2013; Wang Y S et al., 2020). At the depth of 5 km, the NE direction is also characterized by high velocity zonation, which is related to the possible existence of high velocity rock mass in the upper crust near the Tudiling-Luoerling fault.

3.2 Low velocity anomaly and seismicity distribution at the intersection of different faults

At the depth of 5–7 km, the intersection of Tudiling-Luoerling and Qingshan-Xiaotian faults presents a relatively low velocity anomaly, and it is concentrated with medium and small earthquakes. The earthquake relocation results (TomoDD, Zhang and Thurber, 2003) show that small earthquakes in the Huoshan area exhibit obvious NE
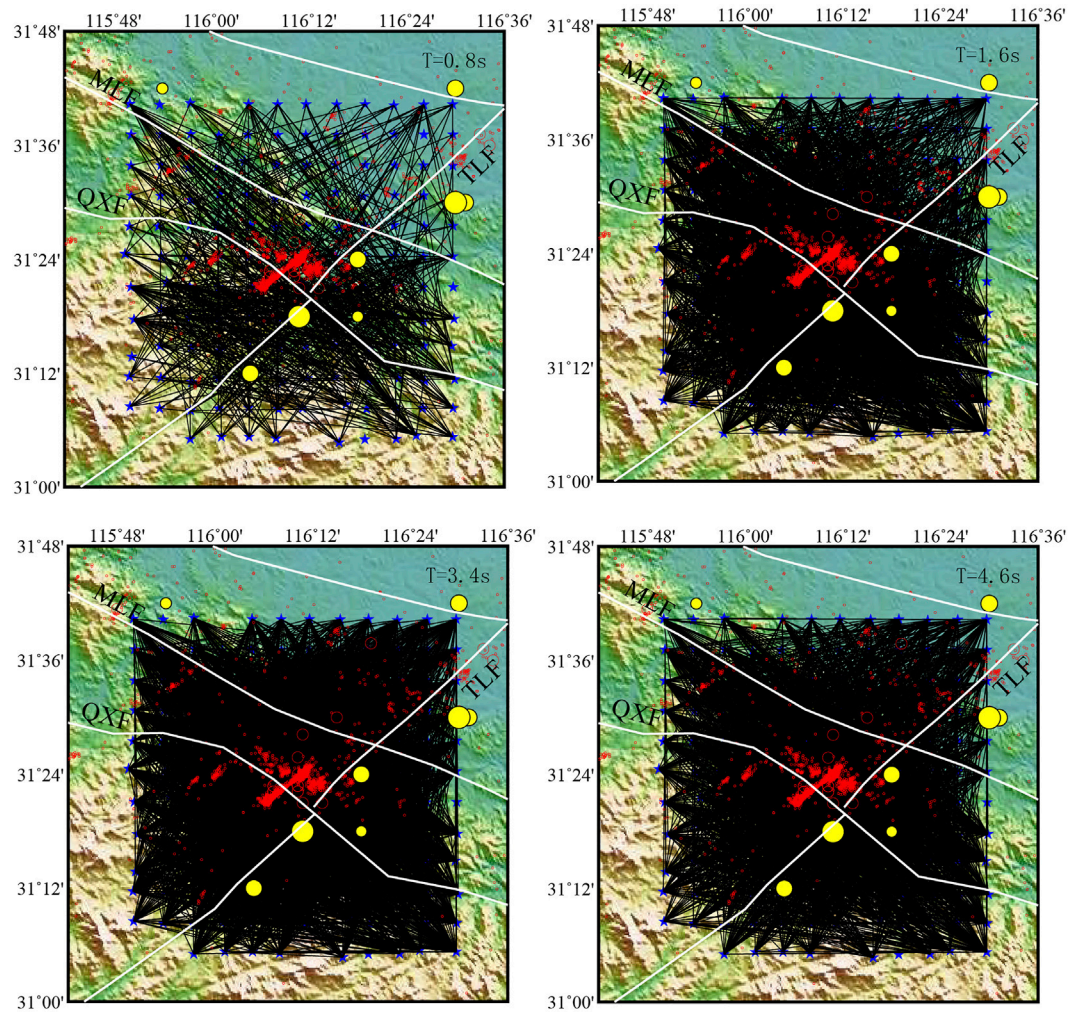
FIGURE 7
Distribution of the ray-path covered in Huoshan and adjacent area (T = 1,2,3,4,5,7 s). Red dots and circles represent the relocated earthquakes have been occurred during 2010−2022 and yellow circles are the same shown in Figure 2.

and NW banded distribution (Figures 8A, F). The dominant depth after positioning is mainly 5–10 km, which is basically located in the low velocity area. The NE-trending strip has a high degree of seismic concentration, and its strike is similar to that of the Tudiling-Luoerling fault. The NW-trending strip is along the strike direction of the Qingshan-Xiaotian fault and perpendicular to the Tudiling-Luoerling fault. The figure shows that the two fractures in different directions play an important role in controlling the spatial distribution of earthquakes in the Huoshan area. The relatively broken faults near the intersection area form a tectonic weak zone and extend to the surface, which is consistent with the concentrated small earthquakes.

4 Discussion

4.1 Deep characteristics of main faults on the northern edge of Dabie orogenic belt

Many groups of NW trending faults are present on the northern edge of the Dabie orogenic belt, which intersect with NE-trending

faults and form complex structure features on the surface. The NW-trending faults mainly include the Meishan-Longhekou, Jinzhai-Shucheng, and Qingshan-Xiaotian faults, which are mainly exposed to the surface, and their active age is probably in the early Middle Pleistocene (Zhao et al., 2018). The NE-trending Tudiling-Luoerling fault is a relatively new active fault, and the latest active time is from Pleistocene to early Late Pleistocene (Shu et al., 2018). Figure 9 displays the six vertical profiles along NW and NE directions in the study area, revealing that the crustal velocity structure on the northern edge of the Dabie orogenic belt is closely related to the fault properties.

4.1.1 Qingshan-xiaotian fault

The three vertical velocity profiles of AA', BB' and CC' (Figures 9A–C) along the Dabie orogenic belt from the south to north exhibit obvious boundary characteristics of high and low velocity anomalies at the junction of the mountain and basin. The AA' and BB' profile reveal that the large velocity variation in the shallow crust corresponds to the location of the Qingshan-Xiaotian and Meishan-Longhekou faults. The most significant velocity contrast is argubaly observed beneath the
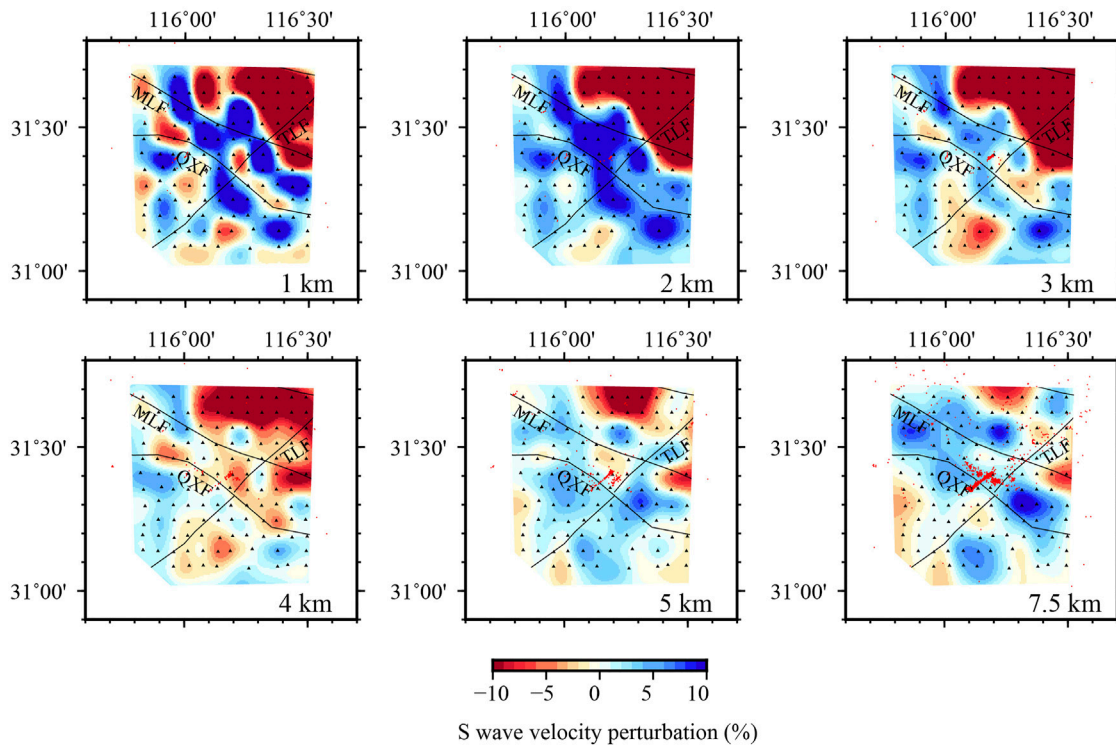
FIGURE 8
Slices of shear wave velocity at the depths of 1–7.5 km (Red dot represents the re-locations of earthquakes below magnitude 3).

Meishan-Longhekou faultand Meishan-Longhekou fault is also known as Jinzhai-Shucheng fault in some geological researches. It is considered that the extensional structure of the Qingshan-Xiaotian fault and the thrust nappe structure with the Jinzhai-Shucheng fault as the front edge have the same shear direction, which is part of the extensional structure during the exhumation of the ultrahigh-pressure metamorphic rocks in the Dabie Mountains (Jiang et al., 2003). This fault separated the Hefei Basin and Dabie mountains (Figure 8, and Figures 9A, C, E), and delineates nicely the northern boundary of the seismogenic zone in Figure 2.

The Qingshan-Xiaotian fault has an anti "S" shape, and the velocity map shows that different sections exhibit different tendencies (Figures 9A, B). The AA' profile shows that the northwest section of the fault under the surface dips toward the northeast and that the high velocity anomaly on both sides is discontinuous (black dash line in Figure 9A). The BB' profile shows that the middle section of the fault tends to be nearly vertical and that the velocity structure on both sides has a slight gradient difference (Figure 9B). The electrical structure of the Dabie orogenic belt shows that (Xiao et al., 2007), under the north inclined and normal Qingshan–Xiaotian fault (Xiang et al., 2008), a relatively high resistivity and conductivity change occurs in the middle and upper crust, which is a boundary fault separating the North Dabie and North Huaiyang massifs. This has been verified by other geophysical integrated explorations (Liu et al., 2003; Yang, 2003; Zhang et al., 2012). Significant velocity variation beneath the north edge of Dabie mountain in this study confirm that the Qingshan–Xiaotian fault and Meishan-Longhekou fault dislocated different strata in the upper crust of the Huoshan area.

According to the research on deep structural characteristics, due to the subduction and collision between the Yangtze plate and North China plate, and due to the strong compression deformation environment in the orogenic process, the dislocation of the Moho under the Qingshan-Xiaotian fault has reached 4.5 km (Wang et al., 1997; Liu et al., 2003). The suture zone between the Yangtze plate and the North China plate may be located below this fault (Yang, 2003; Yuan et al., 2003; Xu et al., 2008). Although the surface location of the suture zone cannot be determined from the shallow crustal structure, the AA 'and BB' profiles still reveal that the Qingshan–Xiaotian fault presents a high shear wave velocity, especially at a depth of 6–8 km where the value is as high as 3.8 km/sThe high velocity structure from the deep suture zone may be related to the upwelling of the upper mantle magma, the remelting of the crustal material, and the local intrusion, occurring during the collision of the two large blocks of the Yangtze and North China.

4.1.2 Tudiling-luoerling fault

Figures 9D–F reveals relatively obvious high and low velocity changes, showing that the dip angle of the Tudiling-Luoerling fault is nearly vertical. The DD ' (Figure 9D) and EE' (Figure 9E) profiles show that the velocity of different sections has significantly changed. The DD' profile reveals that the northeastern segment of the Tudiling-Luoerling fault gradually hides in the Hefei basin at a depth of about 4 km. The EE' profile shows that an obvious low velocity area exists in the fault intersection area, extending to a depth of about 8 km. Projection of the relocated earthquakes on to the velocity profile shows that there are three groups of very close parallel faults existing near the high and low velocity gradient zone
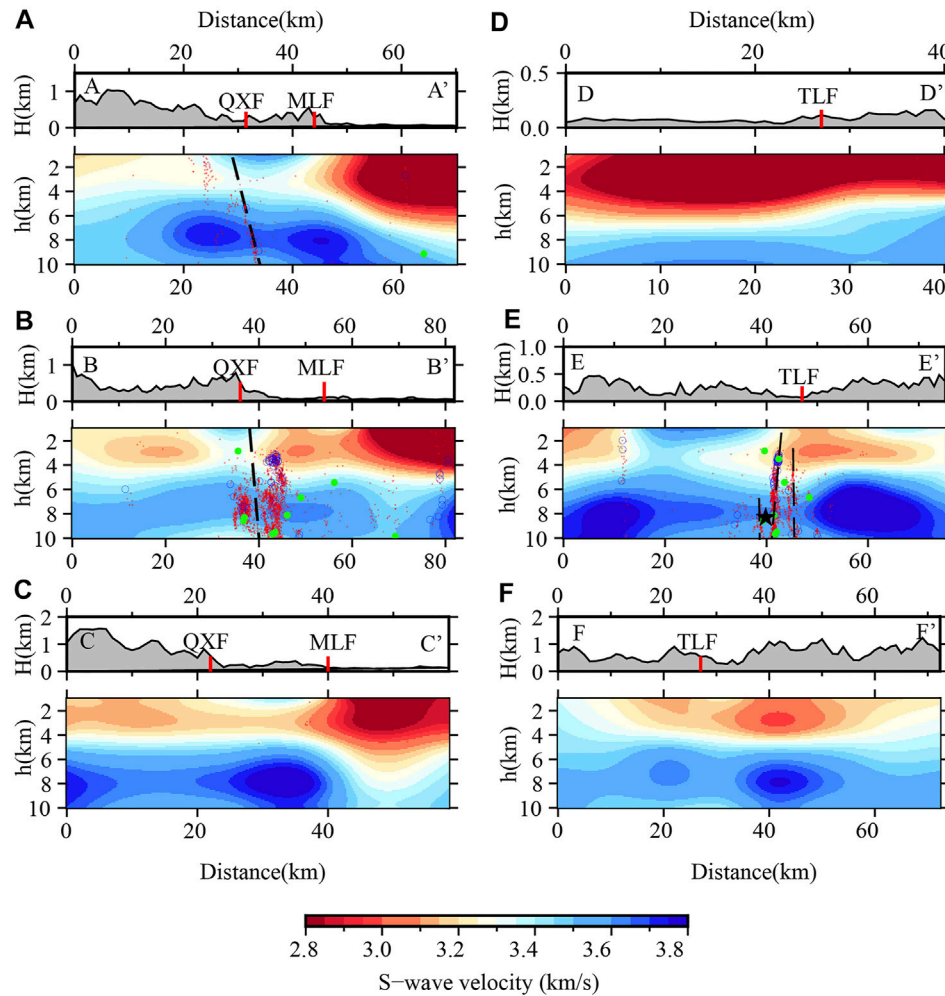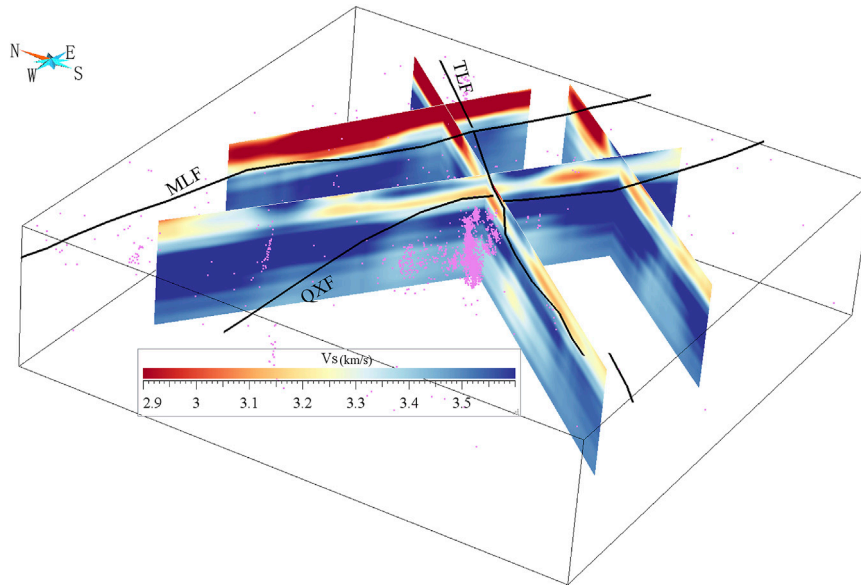
FIGURE 9
Shear wave velocity structure in different vertical profile **(A–F)** shown in Figure 2 (The red and blue circles are the small earthquakes of ML0-1.9, 1.9–2.9, respectively; the green dots represent earthquakes above ML3. The black star represents the 2014 Huoshan M4.3 earthquake. Black dashed lines represent the inferred fault under the surface).

(Figure 9E) and that the seismic concentration of the middle fault is the highest. It is indicated that Tudiling-Luoerling faults is composed of multiple secondary faults in th shallow crust. Xu et al. (2022) used the regional stress field to simulate and calculate the sliding properties of three NE-trending seismic sections in the Huoshan area, which is consistent with the trend of the Tudiling–Luoerling fault andmatches the results of this study. In the late period of the Dabie orogen, a series of extensional faults formed in the Dabie Mountains due to the extensional action in the NS direction (Ma et al., 2003). The NE-trending Tudiling–Luoerling fault inherited the tectonic weak zone of the early Qingshan–Xiaotian fault in the shallow crust in the way of the right-lateral strike–slip (Cui et al., 2020) and formed numerous fault planes with an echelon parallel arrangement with different depths in the low velocity area at the intersection. Xu et al. (2022) suggested that this was related to the pull apart produced by the right-lateral right step of the Tanlu fault zone and the Shangcheng-Macheng fault. By the convergence of the tectonic force, it forms multiple faults and cause large amounts of small earthquakes in the Huoshan area.

4.2 Low velocity and fault seismogenic environment in shallow crust of Huoshan "seismic window"

The main earthquakes in Huoshan "seismic window" are distributed in the low velocity area at a depth of 5–8 km. The deep seismic wide-angle reflection/refraction results of the eastern Dabie (Liu et al., 2003) reveal the high-velocity dome structure in the Dabie Mountains, and a low velocity layer exists in the middle and upper crusts on its wings. Moreover, the tomography results (Xu et al., 2000) reveal that the middle and upper crustal tectonic detachment zone in the Dabie Mountains is the main tectonic reason for the existence of low velocity layers, which is closely related to the deep subduction of the Yangtze Block as well as the collision orogeny and compression uplift of the North China Block. The Qingshan–Xiaotian fault is a large-scale boundary fault that cuts through the crust inside the Dabie Mountains. The profiles across the Qingshan-Xiaotian fault exhibit obvious discontinuous high velocity in the upper crust (Figures 9A, B), inferring the location of the north detachment of the dome wing of the Dabie Mountains is near the Qingshan-Xiaotian fault, which is

FIGURE 10
3-Dimensional map of the upper crust structure with the distribution of small earthquakes in Huoshan "seismic window" (Black lines on the surface are the known faults, and pink dots are the earthquake swarm).

consistent to the observation of the seismic wide-angle reflection/refraction (Liu et al., 2003).

Figure 10 displays multiple profiles of the earthquakes by combining multiple profiles. The relatively low velocity zone to the north at the intersection of the Tudiling-Luoerling fault and the Qingshan-Xiaotian faults is also a concentrated area of earthquakes. The electrical structure suggests that the earthquake cluster area is located in a relatively high conductivity area, which is related to the truncation of the fluid in the high conductivity layer of the middle and lower crust, migration to both sides under the compression environment, rising through the fault, and weakening of the stress conditions (Xiao et al., 2007; Cui et al., 2020). From the position of the low-velocity body, this area may be interpreted as the low velocity detachment zone at the wing of the Dabieshan dome. A structural weak zone formed under the action of multiple sets of faults. Since large amounts of strain cannot be accumulated, small earthquakes are active and concentrated. Multiple en echelon parallel secondary faults (black dashed lines in Figure 9E) of the Tudiling-Luoerling fault zone in the upper crust are all near the low velocity zone, which plays a major role in controlling the concentrated activity of NE-trending small earthquakes.

Historical earthquakes with magnitudes of over 5 are mainly distributed along the Tudiling-Luoerling fault in the NE direction, which is different from the concentrated distribution of small earthquakes at the fault intersections. This study discussed the reasons for the difference of spatial distribution between historical and modern small earthquakes. The BB' section (Figure 9B) shows that small earthquakes below ML3 are mostly concentrated on both sides of the Qingshan-Xiaotian fault, forming two obvious clusters of seismic activity. One of the main fault planes to the north side controls most of the seismic activity. However, the seismicity above ML3 is not concentrated, and it is scattered along the Tudiling-Luoerling fault to the northeast, denoting that the Qingshan-

Xiaotian fault mainly controls the microseismicity below ML3. Moreover, the surface topography shows that the distribution width of this fault is wide. Considering the distribution of the relocated earthquakes, it can be deduced that there exists several secondary faults in this area. Field geological investigations have determined that the Qingshan-Xiaotian fault leads to ductile shear zones and brittle faults, with the widest ductile shear zone up to 2 km (Wang et al., 2009). The abundant micro-seismic activities below ML1 (Stanek F, et al., 2014) are more likely related to shear slips on micro-fractures on multiple fault planes (Hubbert and Rubey, 1959). The focal depth of earthquakes above ML3 is generally 6–10 km, which is obviously different from the distribution depth of with ML1 and ML2 earthquakes. These larger earthquakes mainly distribute far away from the low velocity weak zone (Figure 9C), which is believed that these areas can accumulate more strain. Figure 9E shows that compared to the more divergent microseismic activity near the Qingshan-Xiaotian fault, the earthquakes especially the larger earthquakes above ML3, are more concentrated on the multiple parallel secondary faults of the Tudiling-Luoerling fault, indicating that the control effect isstronger.

In 2014, an Ms 4.3 earthquake (black star show in Figure 9E occurred in the Huoshan area, with the epicenter located south of the Qingshan–Xiaotian fault, slightly away from the main area of the small earthquake activity. Although the main earthquake was very close to the fault from the surface projection, the EE' profile showed that it was close to the main fault plane of the Tudiling-Luoerling fault; therefore, the seismogenic structure of this earthquake was the Tudiling-Luoerling fault. The Tudiling-Luoerling fault is an active strike-slip fault that exists since the late Pleistocene, which may be the reason why the historically strong earthquake activities have been mainly distributed along the NE direction and are not concentrated in a certain area.

5 Conclusion

In this study, the fine velocity structure of the upper crust in the Huoshan area was obtained using the continuous ambient noise data procured from a dense array. Furthermore, along with the relocated small seismic events, the fine structural characteristics of the upper crust and the relation of the main faults and their correlation with seismic activity were discussed. The following conclusions were obtained:

(1) A significant high velocity belt anomaly exists in the shallow crust in Huoshan "seismic window", which is consistent with the trend of the NW-trending Qingshan-Xiaotian fault, reflecting that numerous high velocity magmatic rocks and metamorphic rocks ascended and were exposed on the surface under the action of strong metamorphic dynamics in this area. As the boundary fault between the North Dabie and North Huaiyang, the Qingshan-Xiaotian fault dislocated different strata, providing an important channel for the upwelling of the upper mantle magma, the remelting of the crustal granite, and the *in-situ* intrusion under the action of strong extrusion deformation environment in the collision process of the Dabie orogenic belt.

(2) At a depth of 5–7 km in the upper crust, the intersection of the Qingshan–Xiaotian and Tudiling–Luoerling exhibits relatively low velocity characteristics. The high and low velocity gradient zone shown in the velocity profile corresponds to the lower part of the Qingshan–Xiaotian fault, revealing the shape of the detachment zone in the wing of the Dabie dome structure. The shallow low velocity of the north of the fault is believed to inherit the low velocity from the middle crust detachment zone, which is closely related to the deep subduction of the Yangtze block as well as the collision orogeny and compression uplift of the North China block.

(3) The low velocity zone of the upper crust in Huoshan "seismic window" is consistent with the main distribution layer of small earthquake activity. The relocated earthquakes exhibit a concentrated and orthogonal zonal distribution on the surface, which is obviously controlled by the NW-trending Qingshan-Xiaotian fault and the NE-trending Tuling-Luoerling fault. Along with the velocity structure and positioning results, the two fault zones are believed to be composed of multiple secondary faults, which are distributed at different depths in the shallow crust. Among them, three parallel and nearly vertical en echelon secondary faults are present in the Tudiling-Luoerling fault zone, which control the occurrence of most earthquakes in Huoshan "seismic window".

Data availability statement

The raw data supporting the conclusion of this article will be made available by the authors, without undue reservation.

References

Bensen, G. D., Ritzwoller, M. H., Barmin, M. P., Levshin, A. L., Lin, F., Moschetti, M. P., et al. (2007). Processing seismic ambient noise data to obtain reliable broad-band surface wave dispersion measurements. *Geophys. J. Int.* 169 (3), 1239–1260. doi:10.1111/j.1365-246x.2007.03374.x

Author contributions

LL completed the main part of the paper, HY provide important suggestions in inversion calculation and result discussion, BZ completed earthquake relocated work, JuL and JiL completed array layout, XW and DZ participated in part of the calculation, and PS, YY and PZ participated in result discussion and map drawing.

Funding

Acknowledgments

Conflict of interest

The authors declare that the research was conducted in the absence of any commercial or financial relationships that could be construed as a potential conflict of interest.

Publisher's note

All claims expressed in this article are solely those of the authors and do not necessarily represent those of their affiliated organizations, or those of the publisher, the editors and the reviewers. Any product that may be evaluated in this article, or claim that may be made by its manufacturer, is not guaranteed or endorsed by the publisher.

Supplementary material

The Supplementary Material for this article can be found online at: https://www.frontiersin.org/articles/10.3389/feart.2023.1110061/full#supplementary-material

SUPPLEMENTARY FIGURE S1
The standard deviation of residuals obtained after 5 iterations is given 686 by the red lines in **(A)**, with a significant convergence after the first 2 iteration and reduction of 687 standard deviations of residuals from 0.48 s to 0.192 s **(B)**.

Cui, T. F., Cen, X. B., Zhan, Y., Zhao, L. Q., and Liu, Z. Y. (2020). Characteristics of deep electrical structure and seismogenic structure beneath Anhui Huoshan earthquake area. *Chin. J. Geophys. (in Chinese)* 63 (1), 256–269. doi:10.6038/cjg2019M0458

Dong, S. W., Gao, R., Li, Q. S., Liu, X. C., Qian, G. H., Huang, D. D., et al. (2005). A deep seismic reflection profile across a foreland of the Dabie orogen. *Acta Geological Sinica (in Chinese)* 79 (5), 595–601. doi:10.3321/j.issn:0001-5717.2005.05.003

Du, J. G., and Zhang, P. (1999). Mesozoic volcanic rocks in northern part of Dabie orogenic belt. *Geoscience*, 57–65.

Fang, H., Zhang, H. H., Huang, Y. C., and van der Hilst, R. D. (2015). Direct inversion of surface wave dispersion for three-dimensional shallow crustal structure based on ray tracing: Methodology and application. *Geophys. J. Int.* 201, 1251–1263. doi:10.1093/gji/ggv080

Han, S., Zhang, H., Xin, H., Shen, W., and Yao, H. (2022). USTClitho2. 0: Updated unified seismic tomography models for continental China lithosphere from joint inversion of body-wave arrival times and surface-wave dispersion data. *Seismological Research Letters* 93 (1), 201–215. doi:10.1785/0220210122

Hong, D. Q., Wang, X. Z., ChengX, et al. (2013). Study on variation of seismic coda Qc value of repeating earthquake series in Anhui "Huoshan Seismic Window". *Chinese Journal of Geophysics (in Chinese)* 56 (10), 3416–3424. doi:10.6038/cjg20131017

Hubbert, M. D., and Rubey, W. W. (1959). Role of fluid pressure in mechanics of over thrust faulting. *Geological Society of America Bulletin* 70, 115–205. doi:10.1130/0016-7606(1959)70[115:rofpim]2.0.co;2

Jiang, L. L., Wu, W. P., Chu, D. R., Liu, Y. C., and Zhang, Y. (2003). Extension-thrust nappe structure in the northern Dabie mountains after the plates collision of mesozoic crustal transition from compression to extension in the Dabie mountains: Evidence from granite. *Chin. Sci. Bull.* 48 (14), 1557–1563. doi:10.1360/csb2003-48-14-1557

Jiang, L. L., Wu, W. P., Hu, L. J., Liu, Y. C., and Su, W. (2000). Tectonic setting of the north Dabie complex in the Dabie mountains. *Geoscience, Journal of Graduate School, China University of Geosciences* 14 (1), 29–36.

Liu, F. T., Xu, P. F., Liu, J. S., Yin, Z. X., Qin, J. Y., Zhang, X. K., et al. (2003). The crustal velocity structure of the continental deep subduction belt: Study on the eastern Dabie orogen by seismic wide-angle reflection/refraction. *Chinese Journal of Geophysics (in Chinese)* 46 (3), 366–372. doi:10.3321/j.issn:0001-5733.2003.03.014

Liu, Y. C., Li, Y., Liu, L. X., Gu, X. F., Deng, L. P., and Liu, J. (2013). Neoproterozoic igneous rocks of triassic low-grade metamorphism in the Dabie orogenic belt: Sheets detached and exhumed from the surface of subducted continental crust. *Chinese Science Bulletin* 58 (23), 2330–2337. doi:10.1360/972013-581

Liu, Y. C., Liu, L. X., Gu, X. F., Li, S. G., and Liu, J. (2010). Discovery of neoproterozoic epimetamorphic granites in the western part of the North Huaiyang belt of the Dabie mountains and its tectonic significance. *Chinese Science Bulletin* 55 (24), 2391–2399. doi:10.1360/csb2010-55-24-2391

Liu, Z. M., Huang, X. L., and Ni, H. Y. (2015). Seismogenic structure of the 20, April, 2014Huoshan Ms4.3 earthquake in auhui region. *Acta Seismologica Sinica* 37 (3), 402–410. doi:10.11939/jas.2015.03.003

Luo, S., Yao, H. Y., Li, Q., Wang, W., Wan, K., Meng, Y., et al. (2019). High-resolution 3D crustal S-wave velocity structure of the Middle-Lower Yangtze River Metallogenic Belt and implications for its deep geodynamic setting. *Science China Earth Sciences* 62 (9), 1361–1378. doi:10.1007/s11430-018-9352-9

Luo, Y., Xu, Y., and Yang, Y. (2013). Crustal radial anisotropy beneath the Dabie orogenic belt from ambient noise tomography. *Geophysical Journal International* 195 (2), 1149–1164. doi:10.1093/gji/ggt281

Luo, Y., Xu, Y., and Yang, Y. (2012). Crustal structure beneath the Dabie orogenic belt from ambient noise tomography. *Earth and Planetary Science Letters* 313, 12–22. doi:10.1016/j.epsl.2011.11.004

Ma, C. Q., Yang, K. G., Ming, H. L., and Lin, G. C. (2003). Time of mesozoic crustal transition from compression to extension in the dabie mountains: Evidence from granite. *Sci. Chi.(Series D)* 33 (9), 817–827.

Miao, P., Hong, D. Q., Wang, X. Z., Liu, Z. M., and Wang, J. (2014). Dynamic backgrounds of the "huoshan seismic window" and its implications. *Earthquake Research in China* 30 (4), 534–542.

Paige, C. C., and Saunders, M. A. (1982). LSQR: An algorithm for sparse linear equations and sparse least squares. *ACM Transactions on Mathematical Software (TOMS)* 8 (1), 43–71. doi:10.1145/355984.355989

Rawlinson, N., and Sambridge, M. (2005). The fast marching method: An effective tool for tomographic imaging and tracking multiple phases in complex layered media. *Exploration Geophysics* 36 (4), 341–350. doi:10.1071/eg05341

Shu, P., Lu, S., Fang, L. H., Zheng, Y. P., and Shong, F. M. (2018). Preliminary study on geometry structure and activity features of Luo'erling tudiling fault in late quaternary. *Technology for Earthquake Disaster Prevention* 13 (1), 87–97. doi:10.11899/zzfy20180108

Stanek, F., Eisner, L., and Moser, T. J. (2014). Stability of source mechanisms inverted from P-wave amplitude microseismic monitoring data acquired at the surface. *Geophysical Prospecting* 62 (3), 475–490. doi:10.1111/1365-2478.12107

Wang, C. Y., Zheng, J. H., Hu, H. X., Lou, H., Zhang, X. K, Song, S. Y., et al. (1997). The study on the crustal structure of Dabie orogenic belt. *Sci. China* 27 (3), 221–226.

Wang, Y. S., Bai, Q., Tian, Z. Q., and Du, H. (2020). Dating of clastic rocks in the southern margin of hefei basin and its implications for the exhumation of ultrahigh pressure rocks in the Dabie orogenic belt. *Sci. China Earth Sci.* 50 (07), 921–935.

Wang, Y. S., Sheng, Y., Xiang, B. W., and Zhang, C. Y. (2012). Metamorphic pressure of the luzhenguan group in the North Huaiyang low-grade metamorphic belt and its indication for evolution of the Dabie mountains. *Geological review* 58 (05), 865–872. doi:10.16509/j.georeview.2012.05.014

Wang, Y. S., Xiang, B. W., Zhu, G., Chen, W., and Wei, X. (2009). 40Ar-39Ar geochronology. *records for post-orogenic extension of the Xiaotian-Mozitan fault* 38 (5), 458–471.

Xiang, B. W., Wang, Y. S., Li, C. C., Zhu, G., and Shi, Y. (2008). Evolution of the Xiaotian-Mozitan fault and its implications for exhumation of Dabie HP–UHP rocks. *Progress in Natural Science* 18 (6), 713–722. doi:10.1016/j.pnsc.2007.11.020

Xiao, Q. B., Zhao, G. Z., Zhan, Y., Chen, X. B., Tang, J., and Wang, J. J. (2007). A preliminary study on electrical structure and dynamics of the ultra-high pressure metamorphic belt beneath the Dabie Mountains. *Chinese Journal of Geophysics* 50 (3), 812–822.

Xin, H., Zhang, H., Kang, Gao, L., and Gao, J. (2019). High-resolution lithospheric velocity structure of continental China by double-difference seismic travel time tomography. *Seismological Research Letters* 90 (1), 229–241. doi:10.1785/0220180209

Xiong, C., Xie, Z. J., Zheng, Y., Xiong, X., Ai, S. X., and Xie, R. X. (2019). Rayleigh wave tomography in the crust and upper mantle of the Dabie-Tanlu orogenic zone. *Seismology and Geology* 41 (1), 1–20. doi:10.3969/j.issn.0253-4967.2019.01.001

Xu, P. F., Liu, F. T., Wang, Q. C., Cong, B. L, Chen, H., and Sun, R. M. (2000). Seismic tomography beneath the Dabie-Sulu collision orogen-3D velocity structures of lithosphere. *Chinese Journal of Geophysics(in Chinese)* 43 (3), 377–385. doi:10.3321/j.issn:0001-5733.2000.03.011

Xu, S. T., Yuan, X. C., and Wu, W. P. (2008). New geological interpretation of the seismic reflection profile from Huangshi to Liu'an across the Dabie Mountains, China. *Geological Bulletin of China* 27 (1), 19–26.

Xu, X., Wan, Y. G., Feng, G., Li, X., Liu, Z. M., and He, J. (2022). Study on three seismic fault segments and their sliding properties revealed by clustered seismic events in Huoshan area, Anhui province. *Chinese Journal of Geophysics* 65 (5), 1688–1700. doi:10.6038/cjg2022P0768

Yang, W. C. (2003). Deep structures of the east Dabie ultrahigh pressure metamorphic belt. *East China. Science in China Series D-Earth Science* 2003 (06), 183–194. doi:10.6038/cjg2022P0768

Yao, D. Q., Liu, J. C., Li, J., and Zhai, H. T. (2003). Seismic activities and structures of the Lu'an-Huoshan seismic risk area. *Seismology and Geology* 25 (2), 211–219. doi:10.3969/j.issn.0253-4967.2003.02.005

Yao, H., Gouedard, P., Collins, J. A., McGuire, J. J., and van der Hilst, R. D. (2011). Structure of young East Pacific Rise lithosphere from ambient noise correlation analysis of fundamental- and higher-mode Scholte-Rayleigh waves. *Comptes Rendus Geoscience* 343 (8-9), 571–583. doi:10.1016/j.crte.2011.04.004

Yao, H. (2020). Building the community velocity model in the Sichuan-Yunnan region, China: Strategies and progresses.2020. *Science China Earth Science* 63, 1425–1428. doi:10.1007/s11430-020-9645-3

Yao, H., van der Hilst, R. D., and de Hoop, M. V. (2006). Surface-wave array tomography in SE tibet from ambient seismic noise and two-station analysis: I - phase velocity maps. *Geophys.J. Int.* 166, 732–744. doi:10.1111/j.1365-246X.2006.03028.x

Ye, Q. D., Ding, Z. F., Zheng, C., Lu, M. M., Wu, P. P., and Chen, H. P. (2015). Phase velocity tomography of Rayleigh and Love waves in Dabie-Sulu and its adjacent areas from ambient seismic noise. *Acta Seismologica Sinica* 37 (1), 29–38. doi:10.11939/jass.2015.01.03

Yuan, X. C., Klemperer, S. L., Teng, W. B., Lai, X. L., and Chetwin, E. (2003). Crustal structure and exhumation of the DabieShan ultra-high pressure oroge, eastern China, from seismic reflection profiling. *Geology* 31 (5), 435–438.

Zhang, H., and Thurber, C. H. (2003). Double-difference tomography: The method and its application to the hayward fault, California. *Bulletin of the Seismological Society of America* 93, 1875–1889. doi:10.1785/0120020190

Zhang, J. D., Yang, X. Y., Liu, C. Z., Zhang, L. L., Li, B., Xu, Y., et al. (2012). The fine deep structure of the northern margin of the Dabie Orogenic Belt from gravity-magnetic-electrical-seismic combination survey. *Chinese Journal of Geophysics (in Chinese)* 55 (07), 2292–2306. doi:10.6038/j.issn.0001

Zhang, Z., Li, Y. K., Lu, D. Y., Teng, J., and Wang, G. (2000). Velocity and anisotropy structure of the crust in the Dabieshan orogenic belt from wide-angle seismic data. *Physics of the Earth and Planetary Interiors* 122 (1), 115–131. doi:10.1016/s0031-9201(00)00190-4

Zhao, P., Li, G., Zhai, H., Tong, Y. L., Zheng, Y. P., and Yang, Y. Y. (2018). A preliminary study on quaternary activity of Qingshan-Xiaotian fault zone in east Dabie area. *Plateau Earthquake Research* 30 (03), 11–16.

Zheng, Z. B., Qing, M., and Li, M. L. (1999). Study on correlation between Huoshan seismic window and occurrence of moderate earthquake of East China. *Journal of Seismology* 1999 (2), 1–9.